

Regulon controlled by the GppX hybrid two component system in *Porphyromonas gingivalis*

T. Hirano^{1*}, D.A.C. Beck^{2,3*}, C.J. Wright¹, D.R. Demuth¹, M. Hackett² and R.J. Lamont¹

¹ Center for Oral Health and Systemic Disease, School of Dentistry, University of Louisville, Louisville, KY, USA

² Department of Chemical Engineering, University of Washington, Seattle, WA, USA

³ eScience Institute, University of Washington, Seattle, WA, USA

Correspondence: Richard J. Lamont, School of Dentistry, University of Louisville, Louisville, KY 40292, USA Tel.: +1 502 852 2112; fax: +1 502 852 6394; E-mail: rich.lamont@louisville.edu

*These authors contributed equally.

Keywords: biofilms; periodontal disease; two component system; RNA-Seq

Accepted 15 September 2012

DOI: 10.1111/omi.12007

SUMMARY

The periodontal pathogen *Porphyromonas gingivalis* experiences a number of environmental conditions in the oral cavity, and must monitor and respond to a variety of environmental cues. However, the organism possesses only five full two-component systems, one of which is the hybrid system GppX. To investigate the regulon controlled by GppX we performed RNA-Seq on a Δ GppX mutant. Fifty-three genes were upregulated and 37 genes were downregulated in the Δ GppX mutant. Pathway analyses revealed no systemic function for GppX under nutrient-replete conditions; however, over 40% of the differentially abundant genes were annotated as encoding hypothetical proteins indicating a novel role for GppX. Abundance of small RNA was, in general, not affected by the absence of GppX. To further define the role of GppX with respect to regulation of a hypothetical protein observed with the greatest significant relative abundance change relative to a wild-type control, PGN_0151, we constructed a series of strains in which the Δ gppX mutation was complemented with a GppX protein containing specific domain and phosphotransfer mutations. The transmembrane domains, the DNA-binding domain and the phosphotransfer residues were all required for regulation of PGN_0151. In addition, binding of GppX to the

PGN_0151 promoter regions was confirmed by an electrophoretic mobility shift assay. Both the Δ GppX mutant and a Δ PGN_0151 mutant were deficient in monospecies biofilm formation, suggesting a role for the GppX-PGN_0151 regulon in colonization and survival of the organism.

INTRODUCTION

Porphyromonas gingivalis, a gram-negative oral anaerobe, is a major pathogen in severe and chronic cases of periodontal diseases (Lamont & Jenkinson, 1998; Byrne *et al.*, 2009). *Porphyromonas gingivalis* inhabits several microenvironments of the oral cavity including the plaque biofilm, the gingival crevicular fluid, and the surface and interior of gingival epithelial cells. These microenvironments present a range of different nutritional and physiological conditions. For example, the organism experiences temperature fluctuations, changes in pH and heme concentrations and varying oxygen levels depending on location and disease status of the host (Lamont & Jenkinson, 1998; Kuboniwa & Lamont, 2010).

Porphyromonas gingivalis possess a variety of virulence factors that enable colonization and persistence in the oral cavity, induce destruction of the structural components of the periodontium, and overcome host

immune surveillance mechanisms. Foremost among these are surface proteins including fimbriae, which mediate attachment to host cells, extracellular matrix proteins and other bacteria, and a family of cysteine proteases, the gingipains, which degrade structural components of the periodontal tissues and immune effector molecules (Lamont & Jenkinson, 1998; Sheets *et al.*, 2008; Yilmaz, 2008; Guo *et al.*, 2010). Nonetheless despite its pathogenic potential, *P. gingivalis* is often found in healthy individuals in the absence of disease (Ximenez-Fyvie *et al.*, 2000). Given that the lifestyle of *P. gingivalis* includes different microenvironments and that pathogenic potential is variable, it is important for the organism to sense its environment and regulate gene and protein expression accordingly. Indeed, *P. gingivalis* differentially expresses a large percentage of its transcriptome and proteome according to external conditions (Xia *et al.*, 2007; Kuboniwa *et al.*, 2009; Hirano *et al.*, 2012; Hovik *et al.*, 2012; Yanamandra *et al.*, 2012). Moreover, individual virulence factors such as the fimbriae and proteases are regulated according to environmental cues (Xie *et al.*, 1997; Curtis *et al.*, 2001).

Two component systems (TCS) are widespread signal transduction systems that enable bacteria to modulate gene expression in response to external stimuli (Beier & Gross, 2006). Typical TCS are comprised of a membrane-anchored sensor histidine kinase and a cytoplasmic response regulator. Activation of the sensor causes autophosphorylation of a histidine residue, which subsequently phosphorylates an aspartic acid residue in the cytoplasmic transcriptional regulator (Beier & Gross, 2006). The *P. gingivalis* ATCC 33277 has only five sensor histidine kinases and six response regulators annotated in the genome (Hasegawa *et al.*, 2003; Naito *et al.*, 2008), whereas in *Escherichia coli* there are 30 histidine kinases (Galperin, 2005) and 39 response regulators (Ashby, 2004), suggesting that the individual *P. gingivalis* TCS may play multiple roles. Indeed, the most extensively studied TCS in *P. gingivalis*, the FimR/FimS system, controls expression of around 10% of the *P. gingivalis* genome, including seven different transcriptional regulators (Lo *et al.*, 2010). Phenotypic properties controlled by FimR/FimS include fimbriation and single species biofilm formation (Nishikawa *et al.*, 2004; Wu *et al.*, 2007; Lo *et al.*, 2010; Nishikawa & Duncan, 2010).

Porphyromonas gingivalis also possess a hybrid TCS, in which the sensor and response regulator domains are contained in the same protein, comprised of the 961 amino acid GppX protein (PGN_1768) (Hasegawa *et al.*, 2003). GppX is predicted to contain a N-terminal membrane-anchored sensor kinase domain and a C-terminal response regulator domain with a helix-turn-helix motif (Hasegawa *et al.*, 2003). The response regulator domain shows homology to the AraC family of DNA-binding proteins. AraC is one of the largest families of regulatory proteins in bacteria responsible for controlling a variety of cellular processes including carbon metabolism, stress responses and virulence (Yang *et al.*, 2011). GppX has been found to regulate the post-translational maturation and localization of the *P. gingivalis* gingipains, and mutants with insertionally inactivated *gppX* are non-pigmented (Hasegawa *et al.*, 2003). GppX also negatively regulates expression of the *luxS* gene and can therefore impact interspecies communication by *P. gingivalis* (James *et al.*, 2006). Orthologs of GppX are found mostly in the Bacteroides class, and one such protein, TF0022 in *Tannerella forsythia*, has been functionally characterized (Niwa *et al.*, 2011). TF0022 upregulates the expression of glycosylation-related genes and may modulate autoaggregation by a post-translational modification of *T. forsythia* cell-surface components. Although specific cases of GppX-based regulation have been defined, the broader regulon controlled by this hybrid TCS is unknown.

Quantitative transcriptional profiling by high-throughput sequencing of complementary DNAs (cDNAs) (deep sequencing) is a powerful technique for the identification of bacterial regulons (Oliver *et al.*, 2009; Perkins *et al.*, 2009; Beck *et al.*, 2011; Isabella & Clark, 2011). Previously, we have interrogated the *P. gingivalis* transcriptome by SOLiD sequencing and examined differential transcript abundance and small non-coding RNA production in a LuxS mutant. In this work, we present an investigation of the GppX regulon of *P. gingivalis* by the same approach. A deletion and substitution analysis of the GppX protein revealed that the transmembrane domains, the DNA-binding domain and the phosphotransfer residues are required for activity. GppX was found to bind to the promoter region of the regulated gene PGN_0151, which is important for biofilm formation by *P. gingivalis*.

METHODS

Bacterial strains and culture conditions

Porphyromonas gingivalis ATCC 33277 parental and mutant strains were cultured in Trypticase Soy Broth supplemented with yeast extract (1 mg ml⁻¹), hemin (5 µg ml⁻¹) and menadione (1 µg ml⁻¹), anaerobically at 37°C. When necessary, erythromycin (10 µg ml⁻¹), or tetracycline (1 µg ml⁻¹) was incorporated into the medium.

Construction of *P. gingivalis* mutants and complemented strains

Deletion of *gppX* was accomplished by replacing the coding region [2nd to 961st amino acid (aa)] with an erythromycin cassette ($\Delta gppX::EM$). Eight hundred base pairs (bp) upstream and 950 bp downstream of the *gppX* coding regions were amplified by polymerase chain reaction (PCR) from *P. gingivalis* genomic DNA (see, primers in Table S1). A 2.1 kb fragment containing the P^{ermF}::ermF region was amplified from pVA3000 (Lee *et al.*, 1996). These three fragments were mixed at equal molar ratio for fusion PCR, and the product was electroporated into electrocompetent cells of wild-type (WT) *P. gingivalis*. Erythromycin resistance colonies were selected, and insertion of the replacement allele was confirmed by sequencing.

For constructing of complemented strains, the *gppX* coding sequences and promoter region (determined by 5'-RACE; rapid amplification of cDNA ends) were cloned into the *fimA* locus on the genome. DNA sequences containing 500 bp upstream and downstream flanking the *fimA* coding region and the P^{tetQ}::tetQ allele were cloned into pUC19. The *gppX* allele harboring 400 bp upstream of the AUG start codon to 400 bp downstream of the stop codon, was inserted into the resulting plasmid to make *fimA* 5':tetQ:gppX:fimA 3', and the construct was confirmed by sequencing. The *fimA* 5':tetQ:gppX:fimA 3' region was PCR amplified and the fragment was electroporated into the $\Delta gppX::EM$ cells for homologous recombination. Colonies were selected with tetracycline and erythromycin, and the strain was confirmed by both PCR and sequencing. Alleles of *gppX* deletion variants: ΔTM (Δ aa 2–410 containing two transmembrane regions and a periplasmic region); ΔHTH (Δ aa 861–961 containing the helix-

turn-helix DNA-binding domain); and point mutation variants in putative phosphorylation residues (H436A, D704A and H436A/D704A) were constructed by using fusion PCR or the QuikChange II XL Site-Directed Mutagenesis Kit (Agilent Technologies, Santa Clara, CA), and cloned into pUC19 by the same procedure used for cloning the WT *gppX* allele. These variant alleles were then introduced into the *fimA* locus in the $\Delta gppX::EM$ strain by the same homologous recombination procedure for the WT complementation strain. All alleles were confirmed by PCR and sequencing.

For deletion of the PGN_0151 gene, the upstream 700 bp, downstream 800 bp, and the erythromycin resistance gene were amplified and fused by PCR. The amplicon was electroporated into the WT strain and selected with erythromycin. Mutant colonies were confirmed by PCR.

Transcriptome analysis

RNA-Seq was performed as described previously (Hirano *et al.*, 2012). The WT control data used in this study were derived from the previous work and all protocols were consistent. Briefly, RNA was isolated by Trizol from *P. gingivalis* WT and $\Delta gppX$ strains cultured to an optical density at 600 nm of 0.5. RNA was treated with Turbo-DNA free (Ambion, Austin, TX) at 37°C for 1 h, and then purified by an RNeasy mini kit (Qiagen, Valencia, CA). 16S and 23S ribosomal RNAs (rRNA) were removed using a MICROBExpress Bacterial mRNA Enrichment Kit (Ambion). Double-stranded cDNAs were synthesized by a SuperScript Double-stranded cDNA synthesis kit (Invitrogen, Carlsbad, CA).

A fragment DNA library was prepared with the SOLiD v3 Plus System (Applied Biosystems, Carlsbad, CA) and as described previously (Hirano *et al.*, 2012). Briefly, sheared cDNA was blunt-ended and ligated to oligonucleotide adaptors P1 and P2. After purification and size selection (150–200 bp), DNA fragments were nick translated and amplified by library PCR primers 1 and 2. The double-stranded DNA library was immobilized onto SOLiD P1 DNA beads, clonally amplified by emulsion-based PCR and P2-enriched and extended with a bead linker by terminal transferase. Beads were deposited on slides and sequenced on a SOLiD v3 Plus Sequencer (Applied Biosystems) at the Interdisciplinary Centre of

Biotechnology, University of Florida. Results were obtained as good and best beads as color space FASTA files. The unpaired reads resulting from SOLiD sequencing of the GppX mutant were aligned to the *P. gingivalis* genomic scaffold and evaluated for differential abundance against WT as described previously (Hirano *et al.*, 2012). Briefly, the color space reads were aligned to the ATCC 33277 scaffold (NCBI GI:188593544) with BWA version 0.5.8 (Li & Durbin, 2009). The alignments were post-processed with SAMtools (Li *et al.*, 2009) and assigned to open reading frames (ORFs) using MySQL. Data were normalized across the WT and GppX mutant data sets using R, and an RPKM (reads per kilobase per million mapped reads; Mortazavi *et al.*, 2008) for each ORF was calculated. Differential abundance was evaluated using *t*-tests and reported as log₂ RPKM ratios. As with our previous study, for purposes of discussion we used a *P*-value cutoff of 0.05 for statistical significance (Hirano *et al.*, 2012). In practice, the strength of observed trends was evaluated in part by examining the data over a wide range of cutoff values.

The differential abundance data (i.e. log₂ ratios and statistical significance values) were further analysed in the context of protein classifications in COG (Tatusov *et al.*, 2000) and pfam (Finn *et al.*, 2010) databases and the predicted pathways from KEGG (Kanehisa & Goto, 2000). The KEGG analysis was carried out by extracting the set of KEGG pathway IDs for *P. gingivalis* and locus tags (i.e. ORF IDs) associated with each using the KEGG web-services. Next, the pathway depiction rendering web-service of KEGG was used to display the log₂ ratio and *P*-value as node outline in red or green and node background as significance (white to grey), respectively. These pathway depictions were manually inspected.

The sequence data have been deposited in the GEO repository (<http://www.ncbi.nlm.nih.gov/geo>), accession numbers GSM844728–GSM844733.

Quantitative RT-PCR

RNAs from various *P. gingivalis* strains were purified under the same conditions as for the transcriptome analysis. The cDNAs were made by the iScript cDNA synthesis kit (Bio-Rad, Hercules, CA) or the High Capacity cDNA Reverse Transcription Kit (Applied Biosystems). Quantitative RT-PCR was performed

as described previously (Hirano *et al.*, 2012) and 16S rRNA was used as an internal control.

5'-Rapid amplification of complimentary DNA ends (RACE)

Total RNA was isolated by Trizol, genomic DNA was removed by Turbo-DNA free, and RNA was purified by an RNeasy mini kit with an on-column DNase I treatment step. 5'-RACE was performed with a First-Choice RLM-RACE kit (Ambion). The PCR fragments were TA cloned into pCR2.1 vector (Invitrogen) and then sequenced for 5' end detection.

GppX Δ TM protein purification

The *gppX* allele was PCR amplified from genomic DNA using primers (see Table S1) designed to delete the two potential transmembrane regions and a periplasmic region (Δ 2nd aa to 410th aa), and the fragment was cloned into pCold I cold-shock protein expression plasmid (Takara Bio, Shiga, Japan). BL21 (DE3)*pCold I-*gppX* Δ TM cells were cold-shocked at 10°C for 1 h, 1 mM IPTG was added and incubated at 37°C for 5 h for protein expression. After cell lysis, 5 mM of β -mercaptoethanol was added to avoid intermolecular disulfide bond formation and recombinant protein was purified with a TALONTM CellThru Resin (Clontech, Mountain View, CA). Protein purity was confirmed by sodium dodecyl sulfate–polyacrylamide gel electrophoresis and the protein was concentrated with a Centricon 30 (Millipore, Billerica, MA). The buffer was exchanged for TBS (10 mM Tris–HCl, 0.8% NaCl, 5 mM β -mercaptoethanol and 1 \times Halt proteinase inhibitor) and protein concentration was measured by the Protein assay reagent (Bio-Rad) with 1 mg ml⁻¹ bovine serum albumin as the standard.

Electrophoretic mobility shift assay

Electrophoretic mobility shift assay (EMSA) was performed using the LightShift chemiluminescent EMSA kit (Thermo Scientific, Rockford, IL) as described previously (Chawla *et al.*, 2010). Biotin-labeled DNA fragments were generated by PCR using 5' or 3' biotin-incorporated primers. Binding reactions contained 20 fmol biotin-labeled DNA, 20 ng ml⁻¹ poly(dIdC), 10 mM Tris–HCl (pH 7.5), 50 mM KCl, 1 mM dithiothreitol, 2.5% glycerol, 0.05% Nonidet P-40, and

5 mM MgCl₂ with varying amounts of GppXΔTM protein and TBS up to a total volume of 20 μl. Binding reactions were performed at room temperature for 30 min. Samples were separated with a 4% non-denaturing polyacrylamide gel in 0.5× TAE buffer and transferred to a nylon membrane (380 mA, 30 min). Biotin-labeled DNA was detected with streptavidin-horseradish peroxidase conjugate and chemiluminescent substrate (Thermo Scientific). To test the specificity of binding, non-biotin-labeled specific competitor or non-specific competitor generated by PCR from *gppX* coding region were added at 200-fold excess amount to the binding buffer and incubated with GppXΔTM protein for 30 min before biotin-labeled DNA was added. For protein phosphorylation, 50 mM acetyl phosphate lithium potassium salt (APLPS) was included in the binding buffer and incubated for 30 min before the DNA target was added.

Monospecies biofilm assay

Monospecies biofilm formation by *P. gingivalis* was quantified by a microtitre plate assay as described previously (Capestany *et al.*, 2006, 2008). Parental and mutant strains in early log phase (2×10^8 cells) were incubated at 37°C anaerobically for 24 h. The resulting biofilms were washed, stained with 1% crystal violet, destained with 95% ethanol and absorbance at 595 nm was measured. Biofilm assays were repeated independently three times with each strain in triplicate and statistical significance was determined by Dunnett analysis.

RESULTS AND DISCUSSION

RNA-Seq analysis of a Δ*gppX* mutant

GppX is a multi-domain hybrid TCS protein. Canonical two-component systems have been extensively studied, but less is known regarding the operation and function of hybrid TCS. To gain insight into the regulon controlled by GppX, we performed RNA-Seq to quantify transcript abundance in WT and Δ*gppX* mutant strains of *P. gingivalis* and to calculate differential abundance. We obtained 73 and 58 million reads for each of two biological replicates of which 52 and 48% were mapped to the genome. As expected, the majority of reads were attributed to rRNA regions with virtually all the rest to predicted ORFs. The mean

reads mapped across all ORFs for coding and rRNA sequences are shown in the Table S2. As shown in the Fig. S1, the biological replicates for the Δ*gppX* RNA-Seq data are in good agreement with each other, with a correlation coefficient for the ORF-level RPKMs between the replicates of 0.99. The complete set of RPKM data for the Δ*gppX* and WT strains are shown in Table S3.

A total of 90 genes (at $P < 0.05$) were differentially expressed in the GppX mutant strain relative to our previously described WT transcriptome (Table 1). The highest log₂ ratio of upregulated genes was 1.38 (approximately 2.5-fold upregulation), whereas the lowest log₂ ratio of downregulated genes was -2.92 (approximately eight-fold downregulation), suggesting that positive regulation by GppX is more potent than negative regulation. Just under one-third of the differentially abundant ORFs were found to be in clusters of two or three directly neighboring or near neighboring genes.

Several genes were selected for further analysis by quantitative RT-PCR to confirm transcriptional regulation by GppX. PGN_0068 (*traD*), PGN_0151 (hypothetical), PGN_0932 (GCN5-related *N*-acetyltransferase) and PGN_0926 (hypothetical) were all found to be significantly downregulated in the Δ*gppX* mutant (Fig. 1), consistent with the RNA-Seq data. Quantitative RT-PCR also confirmed upregulation of *luxS* in the Δ*gppX* mutant ($P < 0.001$), consistent with previous results (James *et al.*, 2006). Although the RNA-Seq data for *luxS* trended up in the Δ*gppX* mutant, it did not reach the level of statistical significance.

Globally, there was no systematic bias in the COG or pfam databases for the differentially abundant genes. Examination of all of the predicted KEGG pathways similarly revealed no global bias, indicating that there is no systematic function of GppX under nutrient replete growth conditions. TCS are often involved in responses to environmental stress (Mascher, 2006; Mascher *et al.*, 2006), and *P. gingivalis* is frequently subjected to oxidative and nutritional stressors (Lewis, 2010; Johnson *et al.*, 2011; Robles *et al.*, 2011). The role of GppX in the response of *P. gingivalis* to stress is currently under investigation. *Porphyromonas gingivalis* contains a number of putative small RNAs (sRNAs) and we have verified the expression of 11 of these (Hirano *et al.*, 2012). None of these non-coding RNAs were

Table 1 Wild-type versus GppX mutant by RPKM method¹

Locus tag	Gene products	Log2 abundance ratio	P-value
PGN_1478	Hypothetical protein	1.38	0.03
PGN_0160	Thiamine biosynthesis protein	1.33	0.01
PGN_1192	DNA-binding protein histone-like family	1.04	0.01
PGN_0460	DNA-binding protein histone-like family	1.00	0.04
PGN_0164	Hypothetical protein	0.96	0.01
PGN_1054	Virulence modulating gene F	0.96	0.02
PGN_0997	Putative deoxyuridine 5'-triphosphate nucleotidohydrolase	0.88	0.04
PGN_1053	Putative phospho-2-dehydro-3-deoxyheptonate aldolase/chorismate mutase	0.88	0.04
PGN_0315	Precorrin-6x reductase/cobalamin biosynthetic protein CbiD	0.86	0.01
PGN_0316	Precorrin-4 C11-methyltransferase	0.86	0.02
PGN_2023	Putative phosphoribosylformylglycinamide cyclo-ligase	0.81	0.03
PGN_1479	Hypothetical protein	0.81	0.01
PGN_1749	Probable NADPH-quinone reductase	0.78	0.02
PGN_2013	Cation efflux system protein	0.77	0.01
PGN_0285	Pyridine nucleotide-disulphide oxidoreductase	0.77	0.02
PGN_0809	Putative TonB protein	0.75	0.05
PGN_1750	Putative 3-deoxy-D-manno-octulosonate cytidyltransferase	0.75	0.04
PGN_2036	Hypothetical protein	0.71	0.02
PGN_2085	Putative Fe-S oxidoreductases	0.70	0.05
PGN_1061	Hypothetical protein	0.68	0.02
PGN_0331	Hypothetical protein	0.67	0.04
PGN_0770	Hypothetical protein	0.67	0.00
PGN_1504	Adenylosuccinate synthetase	0.66	0.05
PGN_1461	Putative spore maturation protein A/B	0.66	0.02
PGN_1493	Hypothetical protein	0.65	0.03
PGN_0683	TonB-linked receptor Tlr	0.65	0.04
PGN_0677	Putative multi antimicrobial extrusion protein MatE	0.64	0.03
PGN_0998	4-hydroxy-3-methylbut-2-en-1-yl diphosphate synthase	0.63	0.03
PGN_0209	Glycyl-tRNA synthetase	0.63	0.01
PGN_0242	Probable glycosyl transferase family 1	0.62	0.03
PGN_0411	Thiol-disulfide interchange protein	0.62	0.00
PGN_2021	Orotidine 5'-phosphate decarboxylase	0.59	0.02
PGN_1788	Carboxyl-terminal processing protease	0.58	0.03
PGN_1815	Hypothetical protein	0.58	0.01
PGN_1505	Putative folylpolyglutamate synthase	0.57	0.03
PGN_0741	TonB-dependent receptor	0.54	0.04
PGN_1463	Probable UbiA prenyltransferase	0.52	0.04
PGN_0833	Probable Holliday junction DNA helicase RuvA	0.49	0.05
PGN_1566	Hypothetical protein	0.48	0.01
PGN_0241	Hypothetical protein	0.47	0.05
PGN_0811	Hypothetical protein	0.45	0.01
PGN_1446	Hypothetical protein	0.44	0.05
PGN_1599	Hypothetical protein	0.44	0.03
PGN_0766	Aminotransferase class V	0.44	0.04
PGN_0622	Penicillin-binding protein	0.43	0.01
PGN_0249	Hypothetical protein	0.42	0.02
PGN_0115	Na translocating NADH-quinone reductase subunit B	0.41	0.01
PGN_1201	Hypothetical protein	0.39	0.01
PGN_0823	NAD-utilizing dehydrogenases	0.38	0.02
PGN_0617	Hypothetical protein	0.37	0.05
PGN_1794	Hypothetical protein	0.36	0.01
PGN_1992	Putative helicase	0.30	0.03

(continued)

Table 1 (continued)

Locus tag	Gene products	Log2 abundance ratio	P-value
PGN_1689	Transketolase	0.18	0.03
PGN_1757	GTP pyrophosphokinase	-0.23	0.03
PGN_0173	Glyceraldehyde 3-phosphate dehydrogenase type I	-0.34	0.04
PGN_0550	Aminomethyltransferase	-0.37	0.00
PGN_0579	Hypothetical protein	-0.40	0.03
PGN_1931	Hypothetical protein	-0.43	0.04
PGN_0885	Probable nitroimidazole resistance protein	-0.50	0.00
PGN_1541	Hypothetical protein	-0.54	0.04
PGN_1987	Hypothetical protein	-0.54	0.04
PGN_1456	Hypothetical protein	-0.56	0.02
PGN_0790	Transposase in ISPg3	-0.66	0.04
PGN_1648	Putative 50S ribosomal protein L21	-0.68	0.02
PGN_1990	Hypothetical protein	-0.68	0.01
PGN_1274	Hypothetical protein	-0.69	0.04
PGN_1066	Transposase in ISPg3	-0.71	0.01
PGN_0955	Transposase in ISPg3	-0.72	0.00
PGN_1181	Probable thiol:disulfide oxidoreductase	-0.73	0.03
PGN_1301	Probable transcriptional regulator	-0.76	0.01
PGN_0106	Partial transposase in ISPg3	-0.78	0.02
PGN_1290	Hypothetical protein	-0.81	0.03
PGN_0531	Putative von Willebrand factor type A	-0.82	0.03
PGN_0306	Hypothetical protein	-0.85	0.02
PGN_1278	Partial transposase in ISPg3	-0.85	0.03
PGN_1911	Transposase in ISPg3	-0.87	0.00
PGN_1591	Hypothetical protein	-0.87	0.05
PGN_1586	Hypothetical protein	-0.96	0.03
PGN_0860	Hypothetical protein	-0.96	0.03
PGN_0068	Hypothetical protein	-1.00	0.05
PGN_0923	Putative DNA primase	-1.11	0.02
PGN_1451	Chaperonin GroES	-1.13	0.01
PGN_1840	50S ribosomal protein L17	-1.13	0.04
PGN_0615	Hypothetical protein	-1.14	0.05
PGN_0480	Partial transposase in ISPg4	-1.17	0.04
PGN_1406	Hypothetical protein	-1.20	0.03
PGN_0851	Hypothetical protein	-1.31	0.04
PGN_0322	Hypothetical protein	-1.39	0.04
PGN_0926	Hypothetical protein	-2.16	0.03
PGN_0151	Hypothetical protein	-2.92	0.04

1Red and green indicate upregulation and downregulation in the $\Delta gppX$ mutant relative to wild-type, respectively. Statistical significant is indicated from dark to light with increasing significance.

differentially regulated in the $\Delta gppX$ mutant, indicating a lack of overlap between the GppX and sRNA regulons.

One documented function of GppX is in the maturation and localization of gingipains (Hasegawa *et al.*, 2003). We did not identify regulation of any genes predicted to be involved with post-translational modifications, suggesting a role for hypothetical pro-

tein(s) is this process. Indeed, products of 37 of the 90 differentially regulated genes were annotated as hypothetical proteins (Table 1), indicating that GppX may have a novel role in regulating gene expression in *P. gingivalis*. Moreover, the three most strongly regulated genes encoded hypothetical proteins and we selected the most strongly differentially expressed gene, PGN_0151, for further study.

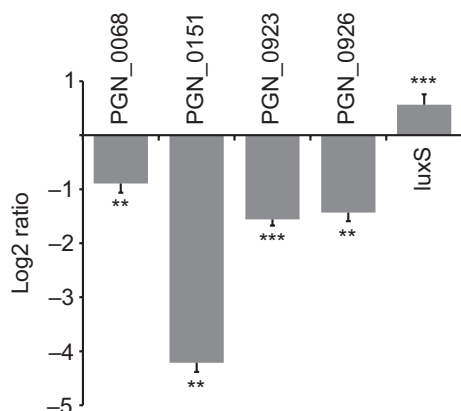


Figure 1 Corroboration of differential gene expression by quantitative reverse transcription-polymerase chain reaction (qRT-PCR). Messenger RNA from wild-type (WT) and $\Delta gppX$ strains was examined by qRT-PCR. 16S ribosomal RNA was used for sample normalization. Significant differences at *** $P < 0.001$ and ** $P < 0.01$ (unpaired *t*-test) in levels of messenger RNA in the $\Delta gppX$ mutant strain in comparison with WT are shown. Data are means with standard deviations of three biological replicates ($n = 9$).

GppX regulation of PGN_0151

The GppX protein is predicted to include an N-terminal periplasmic domain, a histidine kinase domain, a response regulator domain and a C-terminal helix-turn-helix DNA-binding domain. The phosphorylation target residues are H436 and D704 in the kinase domain and the response regulator domain, respectively. To analyze the roles of the domains and phosphorylation status in regulation of PGN_0151, a series of complemented strains were constructed. The large size (13 kb) of pT-COW harboring the WT *gppX* allele prevented transformation of the plasmid into the $\Delta gppX::EM$ mutant. Hence, the *fimA* locus was selected for the insertion site, the rationale being that a number of *P. gingivalis* strains, including W83, are deficient in *fimA* transcription and therefore loss of FimA is unlikely to have a major impact on the phenotype of the organism. Additionally, FimA-mediated adherence events were not under investigation in this study. The downregulation of PGN_0151 was not affected by *fimA* mutation. PGN_0151 expression was recovered to 70% by WT *gppX* complementation; however, none of mutant alleles were capable of restoring expression of PGN_0151 (Fig. 2). These results corroborate both the role of GppX in the regulation of PGN_0151 and the importance of the domain architecture of GppX for regulatory function.

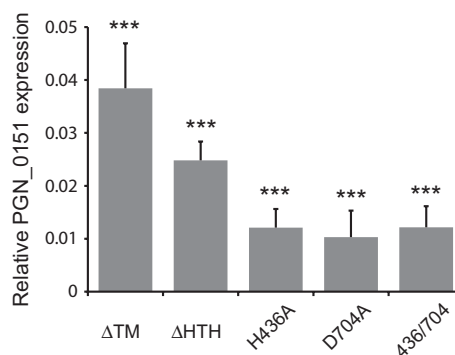


Figure 2 GppX regulation of PGN_0151. Relative gene expression profiles of PGN_0151 in the $\Delta gppX$ strain complemented with various GppX variants relative to complementation with the wild-type *gppX* allele. ΔTM , deletion of the two transmembrane domains; ΔHTH , deletion of the helix-turn-helix DNA-binding domain; H436A, point mutation of alanine for histidine at amino acid (aa) 436; D704A, point mutation of alanine for aspartic acid at aa 704; 436/704, double mutation at aa 436 and 470. Expression levels were normalized by messenger RNA levels of the complemented *gppX* alleles and the ratio to complementation with the wild-type *gppX* allele was calculated. Tukey–Kramer multiple comparison test was used for statistical analysis. *** $P < 0.001$.

GppX binds to the PGN_0151 promoter

To test whether GppX regulation of PGN_0151 is direct, or acts through another *P. gingivalis* regulator, we purified recombinant GppX as a His₆ fusion. To obtain soluble GppX protein for EMSA, we generated truncated protein lacking the two transmembrane regions and putative periplasmic region, designated GppX ΔTM . The RT-PCR data (not shown) indicated that PGN_0152 was the first gene in a two-gene operon containing PGN_0151, and 5'-RACE mapped the transcription start site to 245 bp upstream of the PGN_0152 start codon (Fig. 3). Hence EMSA was performed with the upstream regions of PGN_0152, using PCR-amplified 400-bp fragments, containing about 30 bp of gene coding region. As a control we used the promoter driving expression of *luxS*, which is 5' of the upstream *pfs* gene (Chung *et al.*, 2001). Figure 4 shows that the promoter-containing fragments for both PGN_0151 and *luxS* were completely shifted with 5 μ g GppX ΔTM . The PGN_0151 shift was inhibited by the addition of 200-fold excess amount of unlabeled target DNA, but was unaffected by 200-fold excess amount of DNA fragment amplified from the *gppX*-coding region. Furthermore, a 400-bp fragment from the upstream region of PGN_0151 was not shifted by GppX ΔTM , indicating

```

GATTGAACCG GGGACCTCAT GATTATGAAT CATGCGCTCT AACAGCTGA
GCTATCTCGC CATCGTCTTA CAGTGACATC ATTCATTGTC GCCCTAATTA
AGACGGTGCA AAGGTAGATG TTTTGTGAC ATGCGCAAGA CATCTCTTTT
GTTTTCTTT TCTTGTCTT TCCGCCCTCC TTGGTCCGAG CATCCGCAT
CTCTATCCGA TAGCGAATTG GCCGATCTCT TTTCTTGA AAAGGATACT
TCTCCACGCT CAAAAAGACA TCCGAAAAGA GCTTTTATG ACTTGACTC
GTAATATCTT CTTTATTAGT CTTTACGCG TTTTATG GCGATTGT
CCAAAACGAA GATGTTTTT GTTGTCTCT TATTGCTAAA TCGTGATTT
GTCCAAGAAA ATGCGCGATT TGTCCAAGTA TATCTCCTCG CCACTCCGTT
+1
CCTTTGTGGC AGAGAAGGCC GAACATGCGT TCCGCGTTGT GCGAATTGCC
GATTTTGATT TTGGACACTC TTAGCCAAGG GTAACGATA ATACAATCAG
TAAAAGTAA AAACAAGGAA CGAAAACGCT GAAGAGAGAA TTATGAGCCA
TCGTGCTCTC GTGAAAATAA GATAACAAC TAATCGCTAA TCAACAATTC
AAGAGACTGG AGGGCTCCCG TCCGATCGAG TCTCAAAGAA AAAAAGACAA

PGN_0152
AAACTATGAA GACAAAAGTT TTACGCAAAT TCGTGTGGC GGCTTTCGCC
M K T K V L R K F V V A A F A

GTCGCAACCC TCTGTCTCT CGTCAAGCG CAGACGATGG GAGGAGATGA
V A T L C P L A Q A Q T M G G D D

TGTTAAGGTG GTCCAGTACA ATCAGGAAAA ACTGGTACAA ACGAGGATGA
V K V V Q Y N Q E K L V Q T R M S

```

Figure 3 5' Untranslated region of PGN_0152. The annotated PGN_0153 start and stop codons are shown in bold and as underlined, respectively. The primer used for reverse transcription polymerase chain reaction analysis is highlighted in grey. Part of the PGN_0152 coding region is shown along with the amino acid sequence. The transcriptional start site of PGN_0152 as detected by RACE is shown in bold and designated as +1. Boxed sequences were used as primers for amplifying the electrophoretic mobility shift assay fragment shown in Fig. 4.

specificity of interaction (not shown). Since phosphorylation and dephosphorylation events play an important role in TCS signal transduction, we tested the DNA-binding ability of GppX Δ TM phosphorylated by APLPS. Both phosphorylated and non-phosphorylated GppX bound to the PGN_0151/2 promoter

(Fig. 4). Phosphorylation has been shown to induce dimerization of TCS response regulators and increase binding affinity, although the response regulator can often bind target DNA in the non-phosphorylated state (Dahl *et al.*, 1997). The role of phosphotransfer in hybrid TCS has not been investigated. It may be that the proximity of the response regulator to the histidine kinase results in a conformational change when the phosphate group is present.

Function of PGN_0151

PGN_0151 is annotated as hypothetical; however, its presence has been established by proteomics studies (Xia *et al.*, 2007). The protein possesses a conserved domain of unknown function (DUF3018) that is thought to belong to a family of bacterial lipoproteins; however, no orthologs have been detected in other oral bacteria. We first tested the activity and location of the gingipains in a Δ PGN_0151 mutant and found no difference compared with the parental strain (not shown). As a preliminary investigation into the function of PGN_0151, we then examined the ability of a Δ PGN_0151 mutant to form monospecies biofilms. As shown in Fig. 5, under the conditions tested, the ability of the mutant to form biofilms was reduced compared with the WT. PGN_0151 would therefore appear to be a novel *P. gingivalis* protein with a role in the biofilm lifestyle of the organism.

To summarize, the GppX hybrid TCS of *P. gingivalis* is involved in the regulation of at least 90 genes including 37 genes for hypothetical proteins. One

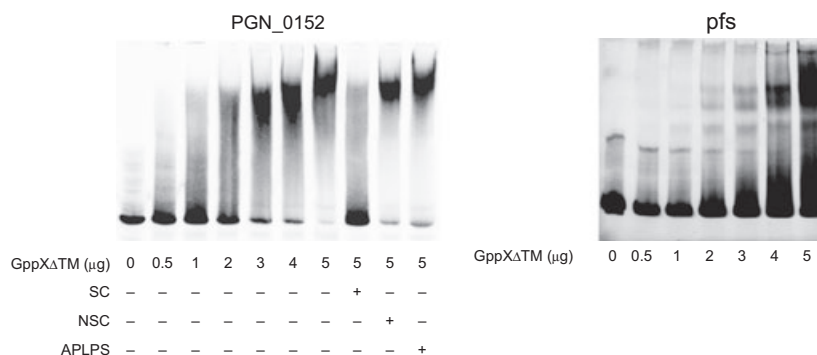


Figure 4 GppX binds to the promoter region of PGN_0151/2. Electrophoretic mobility shift assay was performed with 20 fmol biotin-labeled DNA fragments of the PGN_0151/2 promoter region (left panel) or the *pfs/luxS* promoter as a positive control (right panel). GppX Δ TM protein was used at the concentrations indicated. Non-biotinylated specific competitor (SC) and non-specific competitor (NSC, 200-bp DNA fragment from *gppX* coding region) were used at 200-fold excess molar amounts. APLPS (acetyl phosphate lithium potassium salt) was included where indicated to induce GppX phosphorylation. Image is representative of three independent experiments.

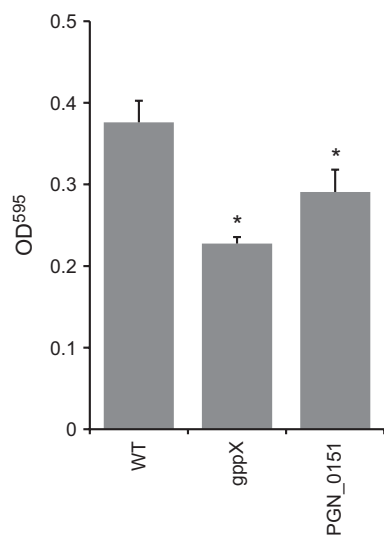


Figure 5 GppX and PGN_0151 regulate homotypic *Porphyromonas gingivalis* biofilm formation. Microtitre plate biofilms of wild-type (WT), $\Delta gppX$ and ΔPGN_0151 after 24 h were stained with crystal violet which was then released with 95% ethanol. Biofilm accumulation was measured by absorbance at 595 nm. * $P < 0.01$ (Dunnett analysis) compared with WT.

such hypothetical protein known to be expressed at high abundance when GppX is present, PGN_0151, is co-transcribed with the upstream gene PGN_0152 and GppX can bind to the promoter region of this operon. PGN_0151 plays a significant role in homotypic biofilm formation by *P. gingivalis*, and the details of that role remain an object of ongoing investigation.

ACKNOWLEDGEMENTS

We thank Erik L. Hendrickson for help with the pathway analysis, and Fred Taub for database programming. This work was facilitated through the use of advanced computational, storage and networking infrastructure provided by the Hyak supercomputer system, supported in part by the University of Washington eScience Institute. The support of the NIDCR through DE14605 (DRD), DE12505 (RJL), and DE14372 (MH) is gratefully acknowledged.

REFERENCES

Ashby, M.K. (2004) Survey of the number of two-component response regulator genes in the complete and annotated genome sequences of prokaryotes. *FEMS Microbiol Lett* **231**: 277–281.

- Beck, D.A., Hendrickson, E.L., Vorobev, A. *et al.* (2011) An integrated proteomics/transcriptomics approach points to oxygen as the main electron sink for methanol metabolism in *Methylobacterium mobilis*. *J Bacteriol* **193**: 4758–4765.
- Beier, D. and Gross, R. (2006) Regulation of bacterial virulence by two-component systems. *Curr Opin Microbiol* **9**: 143–152.
- Byrne, S.J., Dashper, S.G., Darby, I.B., Adams, G.G., Hoffmann, B. and Reynolds, E.C. (2009) Progression of chronic periodontitis can be predicted by the levels of *Porphyromonas gingivalis* and *Treponema denticola* in subgingival plaque. *Oral Microbiol Immunol* **24**: 469–477.
- Capestany, C.A., Kuboniwa, M., Jung, I.Y., Park, Y., Tribble, G.D. and Lamont, R.J. (2006) Role of the *Porphyromonas gingivalis* InlJ protein in homotypic and heterotypic biofilm development. *Infect Immun* **74**: 3002–3005.
- Capestany, C.A., Tribble, G.D., Maeda, K., Demuth, D.R. and Lamont, R.J. (2008) Role of the Clp system in stress tolerance, biofilm formation, and intracellular invasion in *Porphyromonas gingivalis*. *J Bacteriol* **190**: 1436–1446.
- Chawla, A., Hirano, T., Bainbridge, B.W., Demuth, D.R., Xie, H. and Lamont, R.J. (2010) Community signalling between *Streptococcus gordonii* and *Porphyromonas gingivalis* is controlled by the transcriptional regulator CdhR. *Mol Microbiol* **78**: 1510–1522.
- Chung, W.O., Park, Y., Lamont, R.J., McNab, R., Barbieri, B. and Demuth, D.R. (2001) Signaling system in *Porphyromonas gingivalis* based on a LuxS protein. *J Bacteriol* **183**: 3903–3909.
- Curtis, M.A., Aduse-Opoku, J. and Rangarajan, M. (2001) Cysteine proteases of *Porphyromonas gingivalis*. *Crit Rev Oral Biol Med* **12**: 192–216.
- Dahl, J.L., Wei, B.Y. and Kadner, R.J. (1997) Protein phosphorylation affects binding of the *Escherichia coli* transcription activator UhpA to the *uhpT* promoter. *J Biol Chem* **272**: 1910–1919.
- Finn, R.D., Mistry, J., Tate, J. *et al.* (2010) The Pfam protein families database. *Nucleic Acids Res* **38**: D211–D222.
- Galperin, M.Y. (2005) A census of membrane-bound and intracellular signal transduction proteins in bacteria: bacterial IQ, extroverts and introverts. *BMC Microbiol* **5**: 35.
- Guo, Y., Nguyen, K.A. and Potempa, J. (2010) Dichotomy of gingipains action as virulence factors: from cleaving substrates with the precision of a surgeon's knife to a meat chopper-like brutal degradation of proteins. *Periodontol* **2000** **54**: 15–44.

- Hasegawa, Y., Nishiyama, S., Nishikawa, K. *et al.* (2003) A novel type of two-component regulatory system affecting gingipains in *Porphyromonas gingivalis*. *Microbiol Immunol* **47**: 849–858.
- Hirano, T., Beck, D.A., Demuth, D.R., Hackett, M. and Lamont, R.J. (2012) Deep sequencing of *Porphyromonas gingivalis* and comparative transcriptome analysis of a LuxS mutant. *Front Cell Infect Microbiol* **2**: 79.
- Hovik, H., Yu, W.H., Olsen, I. and Chen, T. (2012) Comprehensive transcriptome analysis of the periodontopathogenic bacterium *Porphyromonas gingivalis* W83. *J Bacteriol* **194**: 100–114.
- Isabella, V.M. and Clark, V.L. (2011) Deep sequencing-based analysis of the anaerobic stimulon in *Neisseria gonorrhoeae*. *BMC Genomics* **12**: 51.
- James, C.E., Hasegawa, Y., Park, Y. *et al.* (2006) LuxS involvement in the regulation of genes coding for hemin and iron acquisition systems in *Porphyromonas gingivalis*. *Infect Immun* **74**: 3834–3844.
- Johnson, N.A., McKenzie, R.M. and Fletcher, H.M. (2011) The *bcp* gene in the *bcp-recA-vimA-vimE-vimF* operon is important in oxidative stress resistance in *Porphyromonas gingivalis* W83. *Mol Oral Microbiol* **26**: 62–77.
- Kanehisa, M. and Goto, S. (2000) KEGG: Kyoto encyclopedia of genes and genomes. *Nucleic Acids Res* **28**: 27–30.
- Kuboniwa, M. and Lamont, R.J. (2010) Subgingival biofilm formation. *Periodontol 2000* **52**: 38–52.
- Kuboniwa, M., Hendrickson, E.L., Xia, Q. *et al.* (2009) Proteomics of *Porphyromonas gingivalis* within a model oral microbial community. *BMC Microbiol* **9**: 98.
- Lamont, R.J. and Jenkinson, H.F. (1998) Life below the gum line: pathogenic mechanisms of *Porphyromonas gingivalis*. *Microbiol Mol Biol Rev* **62**: 1244–1263.
- Lee, S.W., Hillman, J.D. and Progulske-Fox, A. (1996) The hemagglutinin genes *hagB* and *hagC* of *Porphyromonas gingivalis* are transcribed in vivo as shown by use of a new expression vector. *Infect Immun* **64**: 4802–4810.
- Lewis, J.P. (2010) Metal uptake in host-pathogen interactions: role of iron in *Porphyromonas gingivalis* interactions with host organisms. *Periodontol 2000* **52**: 94–116.
- Li, H., Handsaker, B., Wysoker, A. *et al.* (2009) The Sequence Alignment/Map format and SAMtools. *Bioinformatics* **25**: 2078–2079.
- Li, H. and Durbin, R. (2009) Fast and accurate short read alignment with Burrows-Wheeler transform. *Bioinformatics* **25**: 1754–1760.
- Lo, A., Seers, C., Dashper, S. *et al.* (2010) FimR and FimS: biofilm formation and gene expression in *Porphyromonas gingivalis*. *J Bacteriol* **192**: 1332–1343.
- Mascher, T. (2006) Intramembrane-sensing histidine kinases: a new family of cell envelope stress sensors in Firmicutes bacteria. *FEMS Microbiol Lett* **264**: 133–144.
- Mascher, T., Helmann, J.D. and Unden, G. (2006) Stimulus perception in bacterial signal-transducing histidine kinases. *Microbiol Mol Biol Rev* **70**: 910–938.
- Mortazavi, A., Williams, B.A., McCue, K., Schaeffer, L. and Wold, B. (2008) Mapping and quantifying mammalian transcriptomes by RNA-Seq. *Nat Methods* **5**: 621–628.
- Naito, M., Hirakawa, H., Yamashita, A. *et al.* (2008) Determination of the genome sequence of *Porphyromonas gingivalis* strain ATCC 33277 and genomic comparison with strain W83 revealed extensive genome rearrangements in *P. gingivalis*. *DNA Res* **15**: 215–225.
- Nishikawa, K. and Duncan, M.J. (2010) Histidine kinase-mediated production and autoassembly of *Porphyromonas gingivalis* fimbriae. *J Bacteriol* **192**: 1975–1987.
- Nishikawa, K., Yoshimura, F. and Duncan, M.J. (2004) A regulation cascade controls expression of *Porphyromonas gingivalis* fimbriae via the FimR response regulator. *Mol Microbiol* **54**: 546–560.
- Niwa, D., Nishikawa, K. and Nakamura, H. (2011) A hybrid two-component system of *Tannerella forsythia* affects autoaggregation and post-translational modification of surface proteins. *FEMS Microbiol Lett* **318**: 189–196.
- Oliver, H.F., Orsi, R.H., Ponnala, L. *et al.* (2009) Deep RNA sequencing of *L. monocytogenes* reveals overlapping and extensive stationary phase and sigma B-dependent transcriptomes, including multiple highly transcribed noncoding RNAs. *BMC Genomics* **10**: 641.
- Perkins, T.T., Kingsley, R.A., Fookes, M.C. *et al.* (2009) A strand-specific RNA-Seq analysis of the transcriptome of the typhoid bacillus *Salmonella typhi*. *PLoS Genet* **5**: e1000569.
- Robles, A.G., Reid, K., Roy, F. and Fletcher, H.M. (2011) *Porphyromonas gingivalis* *mutY* is involved in the repair of oxidative stress-induced DNA mispairing. *Mol Oral Microbiol* **26**: 175–186.
- Sheets, S.M., Robles-Price, A.G., McKenzie, R.M., Casiano, C.A. and Fletcher, H.M. (2008) Gingipain-dependent interactions with the host are important for survival of *Porphyromonas gingivalis*. *Front Biosci* **13**: 3215–3238.
- Tatusov, R.L., Galperin, M.Y., Natale, D.A. and Koonin, E.V. (2000) The COG database: a tool for genome-scale analysis of protein functions and evolution. *Nucleic Acids Res* **28**: 33–36.

- Wu, J., Lin, X. and Xie, H. (2007) *Porphyromonas gingivalis* short fimbriae are regulated by a FimS/FimR two-component system. *FEMS Microbiol Lett* **271**: 214–221.
- Xia, Q., Wang, T., Taub, F. *et al.* (2007) Quantitative proteomics of intracellular *Porphyromonas gingivalis*. *Proteomics* **7**: 4323–4337.
- Xie, H., Cai, S. and Lamont, R.J. (1997) Environmental regulation of fimbrial gene expression in *Porphyromonas gingivalis*. *Infect Immun* **65**: 2265–2271.
- Ximenez-Fyvie, L.A., Haffajee, A.D. and Socransky, S.S. (2000) Comparison of the microbiota of supra- and subgingival plaque in health and periodontitis. *J Clin Periodontol* **27**: 648–657.
- Yanamandra, S.S., Sarrafee, S.S., Anaya-Bergman, C., Jones, K. and Lewis, J.P. (2012) Role of the *Porphyromonas gingivalis* extracytoplasmic function sigma factor, SigH. *Mol Oral Microbiol* **27**: 202–219.
- Yang, J., Tauschek, M. and Robins-Browne, R.M. (2011) Control of bacterial virulence by AraC-like regulators that respond to chemical signals. *Trends Microbiol* **19**: 128–135.

- Yilmaz, O. (2008) The chronicles of *Porphyromonas gingivalis*: the microbium, the human oral epithelium and their interplay. *Microbiology* **154**: 2897–2903.

SUPPORTING INFORMATION

Additional Supporting Information may be found in the online version of this article:

Figure S1. Replicate comparison of per-locus RPKM for coding sequences.

Table S1. Primers used in this study.

Table S2. RNA-Seq coverage statistics.

Table S3. RNA-Seq results of all *P. gingivalis* genes.

Please note: Wiley-Blackwell are not responsible for the content or functionality of any supporting materials supplied by the authors. Any queries (other than missing material) should be directed to the corresponding author for the article.

Copyright of Molecular Oral Microbiology is the property of Wiley-Blackwell and its content may not be copied or emailed to multiple sites or posted to a listserv without the copyright holder's express written permission. However, users may print, download, or email articles for individual use.